Ultraviolet Free-Electron Laser Driven by a High-Brightness 45-MeV Electron Beam

P. G. O'Shea, S. C. Bender, D. A. Byrd, J. W. Early, D. W. Feldman, C. M. Fortgang, J. C. Goldstein, B. E. Newnam, R. L. Sheffield, R. W. Warren, and T. J. Zaugg

APEX Free-Electron Laser Laboratory, MS H825, Los Alamos National Laboratory, Los Alamos, New Mexico 87545

(Received 11 August 1993)

We report on experimental studies of an ultraviolet (UV) free-electron laser (FEL) oscillator driven by low-energy electrons from a radio-frequency linear accelerator. Previous UV FELs have been driven by 350–800-MeV electrons from storage rings. We verify the concept of driving an UV FEL with a low-energy, but high-current, low-emittance electron beam. This and other innovations allowed the FEL to lase at wavelengths from 369 to 380 nm using 45.9–45.2-MeV electrons, and to achieve a peak optical output power of 270 kW. The experimental results are in good agreement with simulations.

PACS numbers: 41.60.Cr, 41.75.Ht, 41.85.Lc

There has been considerable interest in developing free-electron lasers (FELs) as tunable sources of narrow-bandwidth radiation in the ultraviolet (UV, 100–400 nm), extreme ultraviolet (XUV, 10–100 nm), and beyond [1]. In the past, one of the major handicaps of UV FELs was the high energy of the electron beam required to drive the FEL [2,3]. It has been proposed [4] that the development of radio-frequency photocathode sources [5] of high-current, low-emittance electron beams would allow the operation of short-wavelength FEL oscillators in a new low-energy electron beam regime. This Letter describes an experiment to verify this concept.

An FEL oscillator produces coherent light by the combined interaction of an electron beam with the virtual photons of a spatially periodic magnetic field generated by a wiggler, and an optical field stored in a resonator cavity. The lasing wavelength (λ_L) of an FEL scales according to $\lambda_L = \lambda_w(1+a_w^2)/2n_H\gamma^2$, where λ_w is the wiggler period, a_w is the normalized rms vector potential of the wiggler ($a_w = eB\lambda_w/2\pi mc$ where e is the electron charge, m is the electron rest mass, c is the velocity of light, and B is the rms magnetic field of the wiggler), γ is the electron energy divided by mc^2, and n_H is the harmonic number. In an FEL oscillator with a plane-polarized wiggler gain occurs on axis for odd harmonic numbers. Using a value of $n_H > 1$ can lead to lasing at shorter wavelengths if the gain exceeds the resonator losses. Resonator losses are typically a few percent per pass. The gain per pass is determined by a number of variables including the electron beam quality and the design of the wiggler and optical cavity. Heretofore, the primary limiting factor for the lower bound of the lasing wavelength, for a given electron beam energy, was the quality of the electron beam.

While an accurate determination of the gain per pass in an FEL oscillator requires detailed computer simulations [6], Dattoli *et al.* [7] have provided a useful parametrization for the scaling of FEL gain with factors (such as emittance and energy spread) that tend to reduce its value from that of a perfect beam. In the case of an FEL operating in the low-gain Compton regime with an untapered plane-polarized wiggler and where the electron pulse length is much greater than the slippage length ($n_H N\lambda_L$), the small-signal gain (g) scales as

$$g \propto \frac{\hat{I}Q(N,n_H,a_w)}{\gamma[1+F(Na_w\varepsilon_n/\gamma^2\lambda_L)][1+G(n_HN\sigma_E)]}, \quad (1)$$

where $\hat{I}$ is the peak electron beam current, N is the number of wiggler periods, ε_n is the rms normalized transverse emittance of the electron beam ($\varepsilon_n = \pi\beta\gamma[\langle x^2\rangle\langle x'^2\rangle - \langle xx'\rangle^2]^{1/2}$ where x is the transverse coordinate), and σ_E is the rms fractional energy spread of the electron bunch (micropulse). Detailed definitions and discussions of the functions Q, F, and G are given in Ref. [7]. The function $Q(N,n_H,a_w)$ relates to wiggler construction and harmonic number. The functions F and G are gain reduction factors that depend on the electron beam quality. The factor F is zero for a beam with zero emittance and increases quadratically with $Na_w\varepsilon_n/\gamma^2\lambda_L$. Similarly, the factor G is zero for a zero-energy-spread beam and increases quadratically with $n_HN\sigma_E$. In general ε_n is an increasing function of $\hat{I}$. Therefore the gain has a maximum that depends on the relationship between ε_n and $\hat{I}$. Storage-ring-driven FELs [2,3] have operated in the regime of $\hat{I} \ll 100$ A and $\varepsilon_n > 100\pi$ mm mrad. Consequently, in order that the gain overcome the losses, they typically require $\gamma > 700$ for UV lasing. We see from Eq. (1) that an alternative approach is to have $\hat{I}$ large ($\hat{I} > 100$ A), and ε_n small ($\varepsilon_n \ll 100\pi$ mm mrad). The advantage of this approach is that UV lasing can be achieved with low-energy electrons ($\gamma < 100$) by using a higher harmonic ($n_H > 1$) and by using a short-period wiggler.

This approach has been made possible by the recent revolution in the design and construction of low-energy electron linear accelerators [8]. The introduction of radio-frequency photocathode electron guns has allowed the production and rapid acceleration of high-current beams without low-energy drift and bunching sections between the source and the accelerator. This has resulted in beams that have simultaneously high peak current ($\hat{I} > 100$ A) and very low normalized rms emittance

0031-9007/93/71(22)/3661(4)$06.00

($\varepsilon_n < 10\pi$ mm mrad) [9]. Such a low emittance beam allows the use of a wiggler with a much smaller transverse gap than was heretofore possible, resulting in enhanced gain with a small λ_w. Harmonic lasing increases the sensitivity of gain to energy spread [Eq. (1)]. Fortunately electron beams produced by photoinjector linacs have a very small energy spread ($\sigma_E \ll 1\%$) which exhibits only a weak dependence on beam current [8]. In this Letter we describe experiments that demonstrate third harmonic lasing ($n_H = 3$) in the wavelength range from 369 to 380 nm using a 45.9–45.2-MeV range of electron energies. Except for the details discussed below, the configuration of the FEL for the UV experiments was similar to that used for our previous infrared studies and has been extensively described [9]. A description of our previous (unsuccessful) attempts at UV lasing may be found in Ref. [10].

The APEX accelerator [8,9] used for these experiments had an rf photocathode electron source [11]. The electron energy was increased from its nominal value of 40 MeV [9] to 46 MeV for these experiments. The accelerator produced a 40-μs-long macropulse train of 8–15-ps (FWHM) electron micropulses at a 21.7-MHz rate. We have determined an empirical scaling relationship between emittance and current (from 50 to 340 A) for the APEX machine: $\varepsilon_n = [1 + \exp(\hat{I}/k)]\pi$ mm mrad, where the constant $k = 140$ A. By using this expression for ε_n along with the parametrization of Eq. (1), we found that the optimum choice of current for lasing near 375 nm was between 100 and 200 A. Therefore, for the experiments described here, we chose an electron beam peak current of 130 A, which has a corresponding micropulse width of 8 ps FWHM. We measured the energy spread of the electron beam to be 0.24% FWHM averaged over a 20-μs macropulse. Further details of the electron beam properties and measurement techniques may be found in Refs. [8] and [9], and references therein.

The wiggler was a two-block-per-period Halbach design using samarium-cobalt magnets. Our wiggler construction and measurement techniques are described in Refs. [12] and [13]. The minimum wiggler period was achieved by having two blocks (each $5 \times 5 \times 35$ mm) per period and the resulting wiggler period was 13.6 mm. To maximize a_w, and hence to maximize $Q(N, n_H, a_W)$ [Eq. (1)] and the small-signal gain, the wiggler gap was chosen to be the minimum possible subject to the constraint that the vignetting of the optical beam and the electron beam be less than 1%. The diameter of the matched electron beam was approximately 0.4 mm and the diameter of the optical beam at the ends of the wiggler was 0.7 mm. To allow some room for steering and matching the beam into the wiggler, a gap of 1.5 mm was chosen. This gave an rms value of $a_w = 0.58$. The total number of wiggler periods was 73, and was constrained by the 1-m length of the available wiggler housing.

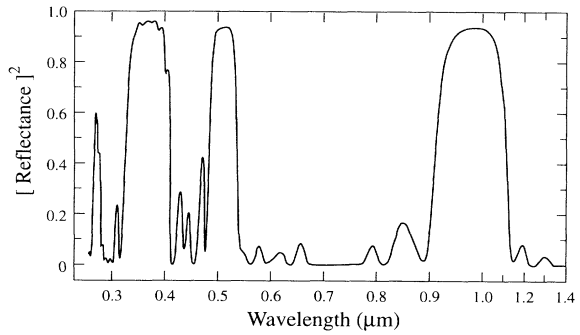

FIG. 1. Cavity mirror reflectance squared (net reflectance for a two mirror cavity) versus wavelength, showing important high reflectance regions near 1000, 527, and 375 nm.

The magnet arrangement chosen had the magnetization vectors parallel and antiparallel to the wiggler axis [12], so as to enhance the gain on the third harmonic. Gain on the third harmonic is derived from two different mechanisms. These two gain mechanisms add or subtract depending on their relative phases [14]. In our case these mechanisms add. If we had chosen an arrangement of blocks where the magnetization vectors were perpendicular to the wiggler axis then the gain mechanisms would subtract. We calculate (using Ref. [14]) that our arrangement enhances the third harmonic gain by approximately 20% over that of the alternative choice.

A near-concentric 6.9182-m linear optical resonator cavity [9] was used for these experiments. The mirrors used were multilayer dielectric (HfO_2 and SiO_2) on Corning fused silica substrates. Light was extracted from the resonator by transmission through the mirrors. The measured reflectance characteristics of the mirrors are shown in Fig. 1. The measurements were made using a Cary wavelength-scanning optical spectrometer and were calibrated using the harmonics of an Nd:YLF laser at 1053 and 351 nm. At 380 nm the measured reflectance of the mirrors was 96.3%, the absorptance was 2.6%, and the net transmittance was 1.1%. These numbers suggest a round-trip cavity loss of approximately 7%. The Rayleigh range was 0.31 m and the empty-cavity waist was at the center of the wiggler.

To improve the quality of the optical alignment for the low-gain third harmonic, the fundamental, with its much higher gain, was used to establish the initial alignments of the optical and electron beam axes, cavity length, and mirror alignment. However, lasing on the third harmonic in the presence of much higher gain on the fundamental set a special requirement for the mirror design; i.e., the fundamental must be suppressed. Therefore the third harmonic and fundamental reflection spectral bands had to differ in wavelength by a factor significantly less than 3. Specifically, we required that the square of the mirror reflectance at 360–380 nm be at least 20 times larger than at 1080–1140 nm. The optimum cavity length

TABLE I. Performance of the FEL at 380 nm.

Electron beam energy (MeV)	45.2
Wavelength (nm)	380
Cavity losses per pass (%)	6.4 ± 0.5
Small signal gain, gross (%)	12.4 ± 1
Cavity detuning length (μm)	17
Macropulse length (μs)	20
Macropulse output power (W)	36 ± 5
Micropulse length (ps)	6 ± 1[a]
Micropulse output power (kW)	270 ± 70
Micropulse intracavity power (MW)	25 ± 6
Extraction efficiency (%)	0.03 ± 0.01

[a]Inferred from calculations.

would be set during fundamental lasing. Then lasing on the third harmonic would be accomplished by a slight downward shift in electron energy. (Note the cavity detuning length was expected to be only a few microns; see below.)

Moderately high reflectance ($\sim$90%) was required at 526.5 nm, the wavelength of the photoinjector drive laser. Injecting the drive-laser light into the FEL resonator and monitoring the multiple-pass ring down facilitated setting the initial resonator length close to the spacing of sequential electron micropulses with an error of less than 100 μm. The optical thin-film code MacLeod [15] was used as an aid in the mirror design. Two reflector stacks were used on each mirror: the upper to reflect 360–380-nm light and the lower to reflect both 526.5-nm and 1-μm light. Using optical multilayer notation, the design between vacuum (V) and substrate (S) was

$$V0.72L(0.36H/0.36L)^8H(1.33L/0.667H)^{10}S,$$

where L and H are quarter-wave optical thicknesses at 1010 nm for SiO_2 and HfO_2, respectively, and the superscripts are the number of layers per stack.

The FEL simulation code FELEX [16] was used to predict the small-signal gain in the experiment. The predicted gross gain was approximately 12%. Assuming cavity losses of 7%, we estimated (using Ref. [17]) that the cavity detuning length (FWHM) would be approximately 2 μm. Using the above mentioned strategy for setting the cavity alignment, lasing was achieved on the fundamental at a wavelength near 990 nm using 47-MeV electrons. Then the electron beam energy was lowered to suppress the fundamental and lase on the third harmonic. Lasing was achieved in the UV at wavelengths from 369 to 380 nm by varying the electron energy from 45.9 to 45.2 MeV. Care was taken to examine the optical spectra of the second harmonic and fundamental during third harmonic lasing. The optical spectrometer showed (after removal of neutral-density filters) that the signal intensity of the fundamental and the second harmonic was 5 to 6 orders of magnitude lower than that of the third harmonic signal and that the spectra were approximately 5% wide. This verified that the mirror design was successful in suppressing lasing on the fundamental.

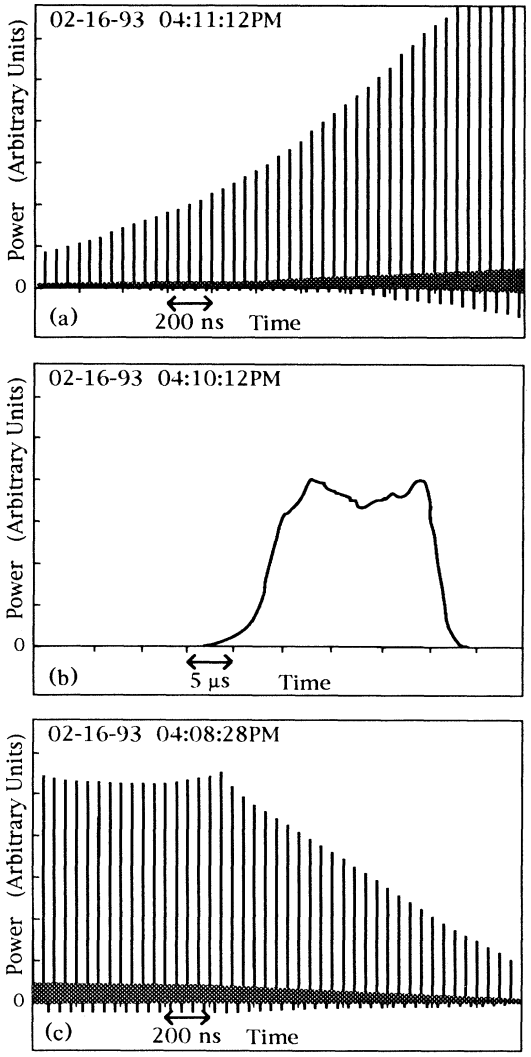

FIG. 2. Vacuum photodiode signals while lasing at 380 nm: (a) laser start-up regime showing individual micropulse signals and net gain of (6 ± 0.5)% per pass; (b) lasing macropulse envelope; (c) cavity ring down after electron beam shutoff, showing cavity losses of (6.4 ± 0.5)% per pass.

Detailed measurements were made at 380 nm and the results are summarized in Table I. Figure 2 shows the optical signals as measured using a vacuum photodiode. The start of the lasing is shown in Fig. 2(a) indicating a net small-signal gain of (6 ± 0.5)% per pass. The macropulse envelope is shown in Fig. 2(b). Lasing was typically achieved over the latter 50% of the electron beam macropulse; i.e., the laser start-up time was approximately 20 μs. The start-up time for lasing as predicted by simulations was 18 μs. The cavity ring down is shown in Fig. 2(c), indicating round trip losses of (6.5 ± 0.5)% per pass. The energy per macropulse extracted from the cavity was measured using a Gentec pyroelectric energy me-

ter. The inferred macropulse-average power extracted from one end of the cavity was 36 ± 5 W. (Note we estimate that an additional macropulse average 85 W was absorbed in each cavity mirror substrate.) The inferred peak power extracted from the cavity was 270 ± 70 kW using an optical micropulse width (derived from simulations) of 6 ps FWHM, and the inferred intracavity power was 25 ± 6 MW using the measured mirror transmittance. The peak intracavity power predicted by simulations was approximately 30 MW. The extraction efficiency of optical power from the electron beam was determined to be $(0.03 \pm 0.01)\%$ compared to the prediction of approximately 0.05% from simulation.

The measured spectral width during lasing was equal to the resolution of the optical spectrometer ($\Delta\lambda/\lambda \approx 4 \times 10^{-3}$). Simulations indicated a spectral width of 2×10^{-3}; however, a spectrometer capable of resolving this was not available. No sidebands were seen and none were predicted by simulation. Simulations predicted the onset of sidebands if the electron macropulse were somewhat longer than 40 μs.

Because the technology was pushed to its limits there were a number of difficulties with the operation of the UV FEL. The small-signal gain was very sensitive to alignment, because the optical beam and the electron beam waist radii were about 200 μm. We found that moving the electron beam off the resonator axis by as little as 100 μm was sufficient to stop the lasing. Tilting one of the cavity mirrors by 5 μrad was sufficient to stop the lasing. The short cavity detuning length was also a problem. The full detuning length (spontaneous to peak power to spontaneous) was approximately 17 μm. The cavity length was measured to change by up to 0.02 μm/s as a result of temperature changes in the FEL vault. A detailed measurement of the detuning curve was not possible because of drifts in the electron beam energy, optical cavity length, and the mirror alignment. The lasing performance was very sensitive to the energy spread of the electron beam. An increase in energy spread of 0.1% was sufficient to stop the lasing. Visible lasing was also achieved on the third harmonic near 510 nm with 39 MeV electrons.

Operation of an ultraviolet FEL driven by a low-energy rf linear accelerator has been demonstrated for the first time. We have verified that a low-emittance, high-current electron beam permits an FEL to operate at short wavelengths with low-energy electrons in agreement with simulations. We believe that a new limit determined by wiggler construction has been approached. If an appropriate shorter-period (7.3 mm) and high-a_w (0.6) wiggler were available, lasing at wavelengths down to 200 nm would be possible with the APEX 46-MeV electron beam. New wiggler options that will be available shortly include superconducting wigglers with iron pole pieces [18] and pulsed electromagnet wigglers [19]. An improved photoinjector accelerator [20] currently under test has produced electron beams whose emittance is 60% that of the APEX machine. These developments are important precursors to FELs that will lase in the extreme UV and beyond.

We thank B. Carlsten, S. Gierman, R. Martineau, K. McKenna, M. Schmitt, and M. Wilke for their assistance and encouragement, and the staff of the APEX FEL Laboratory who kept the machine running. This work was sponsored by the U.S. Department of Energy, Office of Defense Programs.

[1] B. E. Newnam, Proc. SPIE Int. Soc. Opt. Eng. **738**, 155 (1988); V. N. Litvinenko, Nucl. Instrum. Methods Phys. Res., Sect. A **304**, 40 (1991); C. Yamanaka, Nucl. Instrum. Methods Phys. Res., Sect. A **318**, 238 (1992); I. Ben-Zvi *et al.*, Nucl. Instrum. Methods Phys. Res., Sect. A **318**, 201 (1992); C. Pellegrini *et al.*, Nucl. Instrum. Methods Phys. Res., Sect. A **331**, 223 (1993).

[2] G. N. Kulipanov *et al.*, Nucl. Instrum. Methods Phys. Res., Sect. A **296**, 1 (1990).

[3] M. E. Couprie, D. Garzella, and M. Billardon, Europhys. Lett. **21**, 909 (1993).

[4] B. E. Newnam *et al.*, Nucl. Instrum. Methods Phys. Res., Sect. A **318**, 197 (1992).

[5] J. S. Fraser and R. L. Sheffield, IEEE J. Quantum Electron. **23**, 1489 (1987); C. Travier, Part. Accel. **36**, 33 (1991).

[6] J. C. Goldstein, R. W. Warren, and B. E. Newnam, Nucl. Instrum. Methods Phys. Res., Sect. A **304**, 449 (1991).

[7] G. Dattoli, T. Letardi, J. M. J. Madey, and A. Renieri, IEEE J. Quantum Electron. **20**, 637 (1984); **20**, 1003 (1984).

[8] B. E. Carlsten *et al.*, IEEE J. Quantum Electron. **27**, 2580 (1991).

[9] P. G. O'Shea *et al.*, Nucl. Instrum. Methods Phys. Res., Sect. A **318**, 52 (1992); **331**, 62 (1993).

[10] R. W. Warren *et al.*, Nucl. Instrum. Methods Phys. Res., Sect. A **331**, 48 (1993).

[11] D. W. Feldman *et al.*, IEEE J. Quantum Electron. **27**, 2636 (1991).

[12] R. W. Warren and C. M. Fortgang, Los Alamos National Laboratory Report No. LAUR 93-2582 (to be published).

[13] D. W. Preston and R. W. Warren, Nucl. Instrum. Methods Phys. Res., Sect. A **318**, 794 (1992).

[14] M. J. Schmitt and C. J. Elliott, IEEE J. Quantum Electron. **23**, 1552 (1987).

[15] This code may be obtained from H. A. MacLeod, 2745 E. Via Rotunda, Tuscon, AZ 85716.

[16] B. D. McVey *et al.*, Nucl. Instrum. Methods Phys. Res., Sect. A **285**, 186 (1989).

[17] G. Dattoli *et al.*, IEEE J. Quantum Electron. **27**, 2370 (1991).

[18] I. Ben-Zvi *et al.*, Nucl. Instrum. Methods Phys. Res., Sect. A **318**, 781 (1992).

[19] R. W. Warren, Nucl. Instrum. Methods Phys. Res., Sect. A **304**, 765 (1991).

[20] R. L. Sheffield *et al.*, Los Alamos National Laboratory Report No. LAUR 93-3101 (to be published).